ELSEVIER

Journal of Alloys and Compounds 253–254 (1997) 601–604

Journal of ALLOYS AND COMPOUNDS

The hydrogenation characteristics of Ti-Zr-V-Mn-Ni C14 type Laves phase alloys for metal hydride electrodes

H.-H. Lee, K.-Y. Lee, J.-Y. Lee*

Department of Materials Science and Engineering, Korea Advanced Institute of Science and Technology, Kusong-dong 373-1, Yusung-gu, Taejon, 305-701, South Korea

Abstract

In order to develop high discharge capacity negative electrode materials of Ni-MH batteries, Ti-Zr-V-Mn-Ni AB_2 type Laves phase alloys have been developed. In Ti-Zr-V-Mn-Ni alloys with single C14 Laves phase alloys, gaseous hydrogen storage capacities are 1.44–1.71 wt.% H_2 g alloy g^{-1} at 50°C and discharge capacities are 363–464 mAh g^{-1} at a current density of 50 mA g^{-1} at 30°C in proportion to the Ni concentration. However, the cycle life of these alloys were found to be poor. In order to examine the reason for the initial abrupt degradation of Ti-Zr-V-Mn-Ni alloys, surface morphologies, surface concentration profiles and the polarization resistance of the electrodes were investigated. It was found that a Ti-oxide film formed on the degraded electrode surface and the polarization resistance of the degraded electrode increased greatly. These results indicate that the degradation of Ti-Zr-V-Mn-Ni alloys is caused by the Ti-oxide film, which induces an increase of the polarization resistance, including the resistance of the hydrogen diffusion through the Ti-oxide film and the resistance of electron conduction between electrodes and external circuits as well as between alloy particles.

Keywords: Ni-MH; Electrode; Titanium oxide; Discharge capacity; Degradation

1. Introduction

In recent years, increasing attention has been given to Ti-based hydrogen storage alloys as high capacity negative electrode materials of Ni-MH batteries [1–5] because of their high hydrogen storage capacities in comparison with Zr-based and Mm-based metal hydrides. Also their gaseous and electrochemical hydrogenation characteristics can be improved by substituting an alloying element such as Zr, V and Ni. In our previous works concerning Ti-Zr-V-Mn-Ni systems, it was found that the $Ti_{0.2}Zr_{0.05}V_{0.4}Mn_{0.2}Ni_{0.15}$ alloy has a multi-phase structure, which consisted of a C14 Laves phase matrix and a V-rich BCC second phase, as well as a high electrochemical discharge capacity of 440 mAh g^{-1} [5]. There is much room for improvement of the discharge capacity, which can be achieved by adjusting a matrix composition of AB_2 type C14 Laves phase, which has a catalytic ability for charge transfer reactions and a high gaseous hydrogen storage capacity of 1.44 wt.% H_2 g alloy g^{-1}. Also, it is necessary to examine the degradation mechanism of Ti-Zr-V-Mn-Ni alloys because their cyclic properties were poor even though the initial discharge capacities were very high as previously reported [5].

In this study, the matrix phase (AB_2 type Laves phase) of a multi-phase alloy was modified by changing the composition in order to increase the discharge capacity, and its gaseous and electrochemical hydrogenation characteristics were investigated. Also, the degradation mechanism of the Ti-based metal hydride electrode was studied by using scanning electron microscopy (SEM), auger electron spectroscopy (AES) and electrochemical analyses for the degraded electrodes.

2. Experimental details

The Ti-Zr-V-Mn-Ni alloys were prepared by arc melting in an argon atmosphere and were remelted several times in order to ensure the homogeneity of the alloys. These alloys were crushed and grounded into powder mechanically and sieved to -325 mesh in air. To investigate the gaseous hydrogenation characteristics (hydrogen storage capacity and plateau pressure) in a gas–solid reaction, pressure–composition–isotherm (P–C–isotherms) curves were measured by an automatic Sievert's type apparatus at 50°C. Also, in order to identify the crystal structure and the phase of the hydrogen storage alloy, X-ray diffraction (XRD) measurements and SEM analysis were performed.

The metal hydride electrodes were prepared by pressing

---

*Corresponding author.

0925-8388/97/$17.00
PII S0925-8388(96)02930-1

them into a pellet 10 mm in diameter and about 1 mm thick at 5 tons cm^{-2} after mixing 0.2–0.3 g of alloy powder with 10 wt.% nickel powder as a current collector and 10 wt% polytetrafluoroethylene powder as a binder. A half cell was constructed using a platinum wire as a counter electrode and a mercury oxide (Hg/HgO) electrode as a reference electrode in a 30 wt.% KOH electrolyte. The electrodes were charged for 10 h and discharged to −0.7 V vs. Hg/HgO at a current density of 50 mA g^{-1}.

To investigate the surface morphology and concentration profiles of the degraded electrodes after the charging–discharging cycle, SEM and AES analyses were performed respectively. To analyze the degraded electrodes, they were washed out thoroughly using deionized water and then vacuum dried at 60°C. In the AES analyses, a Perkin-Elmer PH14300-SAM instrument having a base pressure of 1×10^{-9} tort was used and a depth profiling was performed by using Ar^{+} ions at 3 kV for sputtering. In order to investigate the polarization resistance of the electrochemical hydrogenation reaction, the linear polarization method was performed on the electrode under the conditions of a 1 mV s^{-1} scan rate and a open circuit potential after discharging to −0.7 V vs. Hg/HgO.

3. Results and discussion

In Ti-Zr-V-Mn-Ni systems, the role of each element is the following as previously reported [5]: the high plateau pressure (above 1 atm) of the Ti-Mn binary alloy falls below 1 atm by substituting V for Mn, Ni should be included in the Ti-V-Mn alloy in order to hydrogenate the alloy in a KOH electrolyte because Ni has a catalytic effect on the charge transfer reaction and Zr is able to increase the reversible hydrogen storage capacity of the Ti-V-Mn-Ni alloy. In this study, in order to increase the discharge capacity of electrode, the matrix phase ($Ti_{0.26}Zr_{0.07}V_{0.24}Mn_{0.2}Ni_{0.23}$) of the $Ti_{0.2}Zr_{0.05}V_{0.4}$-$Mn_{0.2}Ni_{0.15}$ alloy was modified by adjusting the composition based upon the previously stated role of each element. It was found that these alloys had a C14 hexagonal structure and a single phase from the results of the XRD patterns and SEM morphologies. The hydrogenation, electrochemical properties and lattice parameters of the Ti-Zr-V-Mn-Ni AB_2 type Laves phase alloy are listed in Table 1.

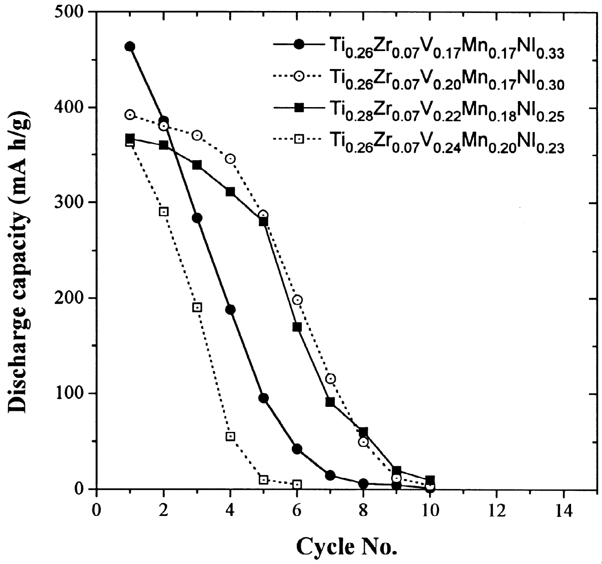

Fig. 1. Cycle life plot of Ti-Zr-V-Mn-Ni alloy with single C14 Laves phase electrode charged and discharged with 50 mA g^{-1} at 30°C: (a) $Ti_{0.26}Zr_{0.07}V_{0.24}Mn_{0.20}Ni_{0.23}$ alloy; (b) $Ti_{0.28}Zr_{0.07}V_{0.22}Mn_{0.18}Ni_{0.25}$ alloy; (c) $Ti_{0.26}Zr_{0.07}V_{0.20}Mn_{0.17}Ni_{0.30}$ alloy; (d) $Ti_{0.26}Zr_{0.07}V_{0.17}Mn_{0.17}Ni_{0.33}$ alloy.

The discharge capacity greatly increases as a function of the Ni concentration, whereas the hydrogen storage capacity increases slightly and the plateau pressure decreases slightly regardless of lattice volume. As a result, the increment of discharge capacities of Ti-Zr-V-Mn-Ni alloys are thought to be attributed to the increment of its catalytic ability on charge transfer reactions on the alloy surface as the Ni concentration increases. In Ti-Zr-V-Mn-Ni AB_2 type Laves phase alloys, it is found that the discharge capacities of these alloys are between 363–464 mAh g^{-1} at 30°C and it seems to be a promising candidate for high capacity negative electrode materials of Ni-MH batteries.

However, although the initial discharge capacities of Ti-Zr-V-Mn-Ni alloys are very high, their cyclic properties are found to be poor. The cycle life plots for these alloys

Table 1
The hydrogenation, electrochemical properties and lattice parameters of Ti-Zr-V-Mn-Ni AB_2 type Laves phase alloys

	C_H (wt.% H_2 g alloy g^{-1})	P_{eq} (atm)	$C_{electro}$ (mAh g^{-1})	Lattice parameter (Å)		Lattice volume (Å^3)
				a	c	
$Ti_{0.26}Zr_{0.07}V_{0.24}Mn_{0.20}Ni_{0.23}$	1.44	4.5	363	4.905	8.018	167.06
$Ti_{0.28}Zr_{0.07}V_{0.22}Mn_{0.18}Ni_{0.25}$	1.71	3	367	5.004	8.168	177.12
$Ti_{0.26}Zr_{0.07}V_{0.20}Mn_{0.17}Ni_{0.30}$	1.61	1.01	392	4.940	8.032	169.75
$Ti_{0.26}Zr_{0.07}V_{0.17}Mn_{0.17}Ni_{0.33}$	1.69	0.72	464	4.918	8.008	167.74

C_H: hydrogen storage capacity calculated from P–C–isotherms curves at 50°C under hydrogen pressure of 50 atm.
P_{eq}: pressure calculated from P–C–isotherms curves at 50°C.
$C_{electro}$: discharge capacity measured from discharge curves at a current density of 50 mA g^{-1} at 30°C.

are shown in Fig. 1. The discharge capacities abruptly decrease within 10 cycles. In order to examine the reason for the initial abrupt degradation of Ti-Zr-V-Mn-Ni alloys, surface morphologies and surface concentration profiles of the electrodes were investigated with electrochemical charging–discharging cycles.

Fig. 2 shows the surface morphologies of the $Ti_{0.26}Zr_{0.07}V_{0.17}Mn_{0.17}Ni_{0.33}$ alloy electrode before cycling (a), after 1 cycle (b), after 3 cycles (c) and after 10 cycles (d) respectively. Before cycling, the shape of the alloy particle and a gap between the alloy powders are distinctly shown. After 1 cycle, it is found that the gap and the shape disappear and a film is formed on the electrode surface, with fine crevices appearing on the surface film. Whiskers are formed on the films after 3 cycles and they are found to be Mn whiskers by energy dispersive spectroscopy (EDS) analysis. After full degradation (10 cycles), these whiskers are found to cover the electrode surface.

In order to examine the film formed on the degraded electrode surface, surface depth profiles of the $Ti_{0.26}Zr_{0.07}V_{0.17}Mn_{0.17}Ni_{0.33}$ alloy electrode were investigated by AES analysis. Fig. 3 shows the depth profile for the constituent elements of the electrode at various stages of cycling. It is found that there is Ti-oxide on top of the surface and a Ni-enriched region at the sub-surface layer after 3 cycles (Fig. 3b). After 10 cycles, there are Mn whiskers on the top surface and a Ti-oxide layer growing thickly into the inner part of the electrode (Fig. 3c). These results clearly prove that the film formed on the degraded electrode is a Ti-oxide layer. The reason why Ti-oxide is formed on the electrode surface is because Ti forms generally stable TiO_2 passive film in alkaline solution unlike other elements [6].

From these results, the initial abrupt degradation of Ti-Zr-V-Mn-Ni alloys is attributed to the formation of Ti-oxide film on the electrode surface rather than the formation of Mn whiskers, because the Ti-oxide film forms on the electrode surface and completely covers the electrode surface in the early stages of cycling, whereas Mn whiskers forms on Ti-oxide films and partially covers the

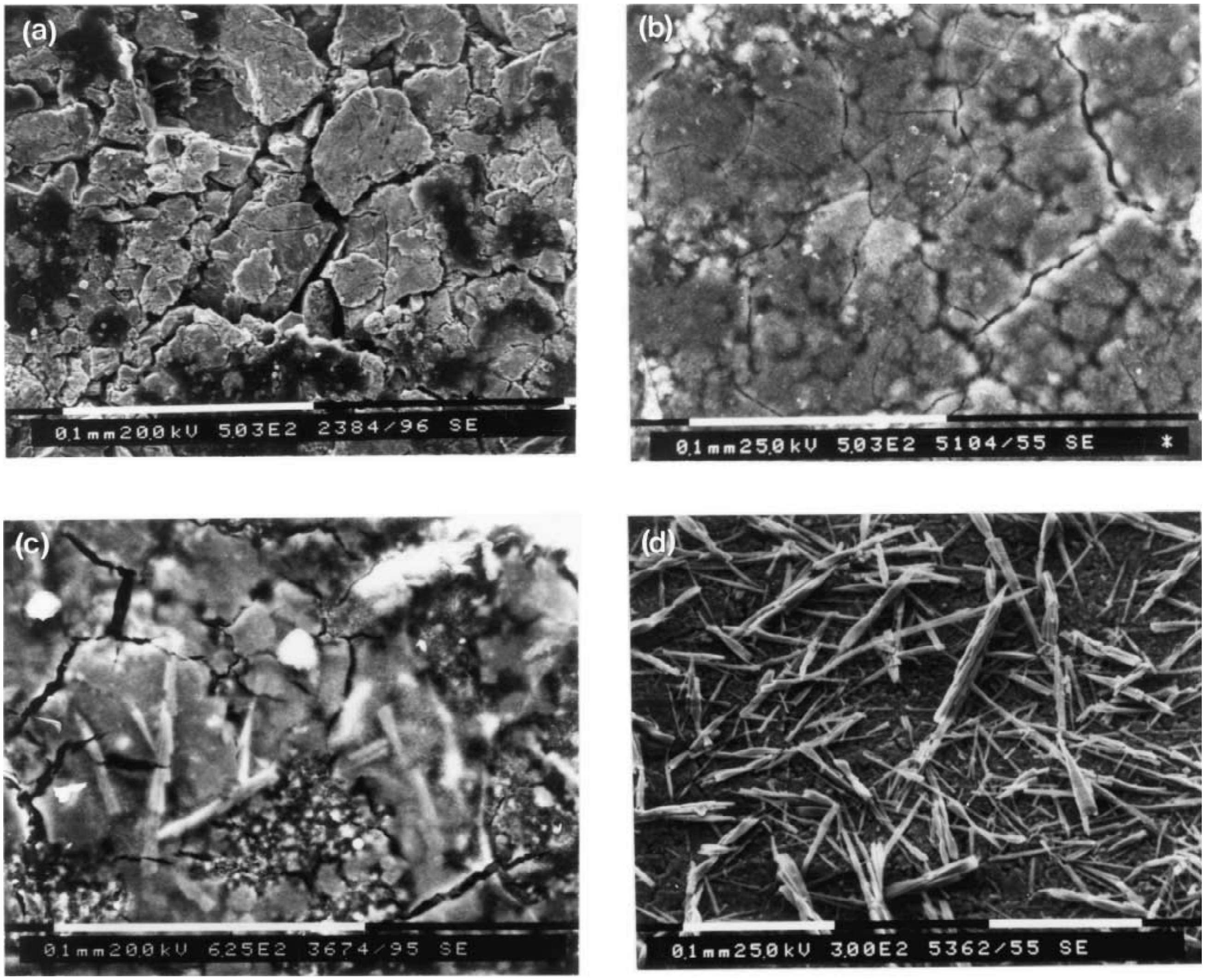

Fig. 2. SEM photographs of the $Ti_{0.26}Zr_{0.07}V_{0.17}Mn_{0.17}Ni_{0.33}$ alloy electrode before cycling (a), after 1 cycle (b), after 3 cycles (c) and after 10 cycles (d).

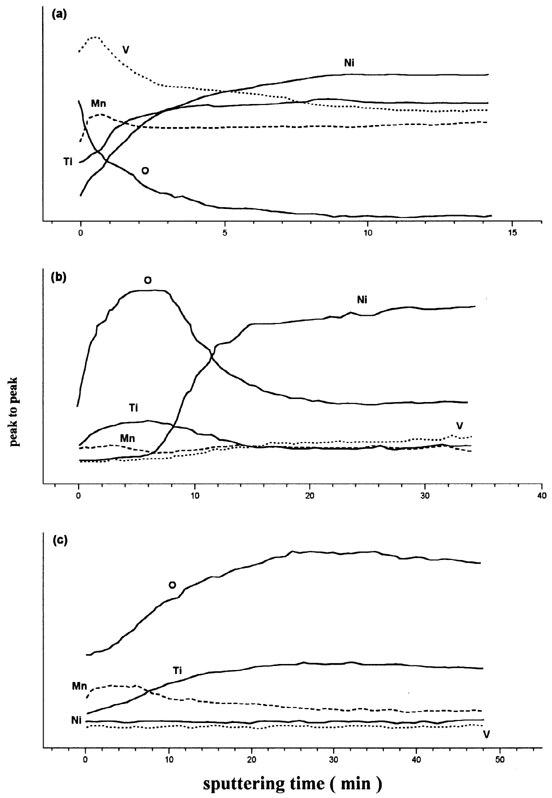

Fig. 3. AES depth profile of $Ti_{0.26}Zr_{0.07}V_{0.17}Mn_{0.17}Ni_{0.33}$ alloy electrode before cycle (a), after 3 cycles (b) and after 10 cycles (c).

electrode surface in the latter stages after the formation of the Ti-oxide film. Also, because Ti-oxide (TiO_2) has a very high electrical resistivity of 10^{11}–10^{12} Ω·m [7] in comparison to 1.4×10^{-6} Ω·m of Mn [8] and a very low hydrogen diffusivity of 10^{-11}–10^{-14} $cm^2\,s^{-1}$ [9], it is hardly hydrogenated through the Ti-oxide film on the electrode surface by a high polarization resistance for the electrochemical hydrogenation reaction.

It is also found that the degraded electrodes have a high polarization resistance in comparison with the initial electrode before cycling and the resistance increases as function of cycle numbers, as shown in Table 2. The polarization resistance of the electrode, which includes reaction resistance, diffusion resistance and contact resistance, was calculated from the overpotential as a function of the applied current by the linear polarization method. The high electrical resistivity of Ti-oxide film induces a large contact resistance for the electron conduction process between electrodes and external circuits as well as between alloy particles. Also, the low hydrogen diffusivity increases the resistance of the diffusion process, which is a transfer reaction of the decomposed hydrogen at the Ti-oxide–electrolyte interface from the Ti-oxide film to the inner part of the electrode in the case of the charging process. Consequently, the high polarization resistance of the degraded electrode is ascribed to the Ti-oxide film formed on the electrode surface.

Table 2
Electrochemical properties of $Ti_{0.26}Zr_{0.07}V_{0.17}Mn_{0.17}Ni_{0.33}$ alloy electrode at various stage of cycling

Cycle number	Discharge (mAh g^{-1})	$E_{i=0}$ (V vs. Hg/HgO)	R_p (Ω·g)
0	-	−0.8392	14.5
1	464	−0.8939	1.8
3	284	−0.8873	7.2
10	10	−0.8124	31.5

From the experimental results and discussion, it seems reasonable to suggest that the degradation of the Ti-Zr-V-Mn-Ni alloy electrode is caused by the Ti-oxide film (TiO_2), which is formed on the electrode surface and has the role of a barrier for electrochemical hydrogenation reaction.

4. Conclusions

In Ti-Zr-V-Mn-Ni systems with C14 Laves single phase, the discharge capacities increase as the content of Ni increases and are in the range of 363–464 mAh g^{-1} and among them the $Ti_{0.26}Zr_{0.07}V_{0.17}Mn_{0.17}Ni_{0.03}$ alloy has the highest electrochemical discharge capacity at 464 mAh g^{-1}. However, it is found that the cycle properties of the Ti-Zr-V-Mn-Ni alloy are very poor and the discharge capacities decrease below 10 mAh g^{-1} before 10 cycles. A cause for the initial abrupt degradation of these alloys is attributed to the formation of Ti-oxide on the electrode surface, thus increasing the polarization resistance for the electrochemical hydrogenation reaction. For these alloys to be applicable to the electrode material of Ni-MH batteries, further work should be done to prevent the formation and growth of the Ti-oxide film, or to break the film in order to improve the cycle life.

References

[1] H.W. Yang, W.S. Lee, Y.Y. Wang, C.C. Wan, T.W. Cheng and K.H. Liang, *J. Mater. Res.*, *10* (1995) 1680.
[2] S. Deying, G. Xueping, Z. Yunshi, Y. Jie and S. Panwen, *J. Alloys Compds.*, *206* (1994) 43.
[3] H. Miyamura, T. Sakai, N. Kuriyama, K. Oguro, I. Uehara and H. Ishikawa, *Zeit. für Phys. Chem.*, *183* (1994) 347.
[4] D.Y. Yah, G. Sandrock and S. Suda, *J. Alloys Compds.*, *223* (1995) 32.
[5] H.H. Lee, K.Y. Lee and J.Y. Lee, *J. Alloys Compds.*, (1996) in press.
[6] M. Pourbaix, *Atlas of Electrochemical Equilibria in Aqueous Solutions*, National Association of Corrosion Engineers, 2400 West Loop South, Huston, TX 77027, 2nd edn, 1974.
[7] J.M. Herbert, *Ceramics dielectrics and capacitors*, Gordon and Breach, New York, 1985.
[8] *Metals Handbook,* Vol. 2, American Society for Metals, OH 44073, 9th edn., 1979.
[9] P. Ruetschi and R. Govanali, *J. Electrochem Soc.*, *135* (1988) 2663.